Available online at www.sciencedirect.com
ScienceDirect
Ceramics International 37 (2011) 1543–1548
CERAMICS INTERNATIONAL
www.elsevier.com/locate/ceramint

Effects of cathode fabrication conditions and cycling on the electrochemical performance of $LiNiO_2$ synthesized by combustion and calcination

Sung Nam Kwon [a,*], Jihong Song [b], Daniel R. Mumm [c]

[a] Department of Hydrogen and Fuel Cells Engineering, Specialized Graduate School, Chonbuk National University, 664-14 Deogjindong 1-ga Deogjingu Jeonju 561-756, Republic of Korea
[b] College of Arts and Sciences, Cornell University, 147 Goldwin Smith, Ithaca, NY 14853, USA
[c] Department of Chemical Engineering and Materials Science, University of California, Irvine, CA 92697-2575, USA

Received 9 September 2010; received in revised form 15 September 2010; accepted 11 January 2011
Available online 18 February 2011

Abstract

$LiNiO_2$ was synthesized by the combustion method with various excess lithium amount z in $Li_{1+z}NiO_2$ (z = 0.04, 0.08, 0.10, 0.12, and 0.15). The sample with z = 0.10 has the largest first discharge capacity of 195 mAh/g at 0.1 C rate and voltage range 2.7–4.4 V with the weight ratio of active material:acetylene black:binder = 85:10:5. The $LiNiO_2$ cathodes, in which the excess lithium amount z for the synthesis of $LiNiO_2$ was 0.10, were fabricated with various weight ratios of active material:acetylene black:binder (85:10:5, 85:12:3, and 90:7:3). The cathode with the ratio of active material:acetylene black:binder 85:10:5 has the best electrochemical properties. The variation, with C-rate, of discharge capacity vs. number of cycles curve for the $LiNiO_2$ cathode with the weight ratio of active material:acetylene black:binder = 85:10:5 was investigated. At 0.1 C rate, the $LiNiO_2$ cathode has the largest first discharge capacity, the discharge capacity degradation rate of 0.70 mAh/g/cycle and a discharge capacity at n = 50 of 134 mAh/g.

Keywords: $LiNiO_2$; Combustion method; Discharge capacity; Cathode fabrication conditions; I_{003}/I_{104}; R-factor

1. Introduction

Transition metal oxides such as $LiMn_2O_4$ [1–3], $LiCoO_2$ [4–6], and $LiNiO_2$ [7–10] have been intensively investigated for their use as cathode materials of lithium secondary batteries. $LiMn_2O_4$ is comparatively inexpensive and does not bring about any environmental pollution, but its cycling performance is not adequate. $LiCoO_2$ has a large diffusivity and a high operating voltage, and it can be easily prepared. However, it has the disadvantage that it contains Co, an expensive element. $LiNiO_2$ is a very promising cathode material since it has a large discharge capacity [11] and is excellent from the economic and environmental viewpoints. On the other hand, its preparation is very difficult compared with $LiCoO_2$ and $LiMn_2O_4$.

It is known that nonstoichiometric $Li_{1-x}Ni_{1+x}O_2$ forms rather than the stoichiometric $LiNiO_2$ during preparation [12] due to cation mixing. Excess nickel occupies the Li sites, destroying the ideally layered structure and preventing the lithium ions from undergoing the easy movement required for intercalation and deintercalation during cycling. This results in a small discharge capacity and poor cycling performance.

$LiNiO_2$ synthesized by the solid-state reaction method does not have a high discharge capacity and has poor cycling performance, probably because it has poor crystallinity and non-uniform particle size distribution. On the other hand, homogeneous mixing of the starting materials is possible in the combustion method because the starting materials are liquid. This may lead to good crystallinity and uniform particle size distribution.

In this work, $LiNiO_2$ was synthesized by the combustion method with various excess lithium amount z in $Li_{1+z}NiO_2$. The $LiNiO_2$ cathodes were fabricated with various weight ratios of active material:acetylene black:binder, and their electrochemical properties were investigated.

2. Materials and methods

The optimum conditions to synthesize $LiNiO_2$ by the combustion method, studied in our previous work [13], were preheating at 400 °C for 30 min in air and calcination at 750 °C

* Corresponding author. Tel.: +82 63 270 2379; fax: +82 63 270 2386.
E-mail address: dasom2u@jbnu.ac.kr (S.N. Kwon).

0272-8842/$36.00
doi:10.1016/j.ceramint.2011.01.028

for 36 h in an O_2 stream. $LiNiO_2$ was synthesized under these conditions. Aldrich Chemical's $LiNO_3$ and $Ni(NO_3)_2{\cdot}6H_2O$ were used as starting materials. Excess lithium was added to compensate for the evaporated lithium during preparation. The excess lithium amount z in $Li_{1+z}NiO_2$ was 0.04, 0.08, 0.10, 0.12, and 0.15. The starting materials, in the desired proportions, were mixed with urea by a magnetic stirrer. The mole ratio of urea to nitrate was 3.6. The heating rate and the cooling rate were about 100 °C/h. The phase identification of the synthesized samples was carried out by the X-ray powder diffraction analysis (Rigaku D/MAX 2500 powder diffractometer) using Cu Kα radiation, scanning rate of 6 °/min and diffraction angle 2θ of $10^\circ \leq 2\theta \leq 80^\circ$. The electrochemical cells consisted of $LiNiO_2$ as a positive electrode, Li foil as a negative electrode, and an electrolyte [Purelyte (Samsung General Chemicals Co., Ltd.)] prepared by dissolving 1 M $LiPF_6$ in an 1:1 (volume ratio) mixture of ethylene carbonate (EC) and diethyl carbonate (DEC). The positive electrode consisted of synthesized materials, acetylene black, and polyvinylidene fluoride (PVDF) binder dissolved in 1-methyl-2-pyrrolidinone (NMP) with weight ratios of 85:10:5, 85:12:3, and 90:7:3. A Whatman glass-filter was used as a separator. The coin-type (2016) cells were assembled in an argon-filled dry box. All of the electrochemical tests were performed at room temperature with a potentiostatic/galvanostatic system. The cells were cycled between 2.7 and 4.4 V at the rates of 0.1 C, 0.2 C, and 0.5 C.

3. Results and discussion

Fig. 1 shows the 1st and 2nd charge–discharge curves of $LiNiO_2$ synthesized with excess lithium $z = 0.08$ at 0.1 C rate in a voltage range of 2.7–4.4 V. This $LiNiO_2$ cathode was fabricated with a weight ratio of active material:acetylene black:binder = 85:10:5. The lengths of plateaus in the charge and discharge curves are proportional to charge and discharge capacities. The first charge capacity is quite larger than the first

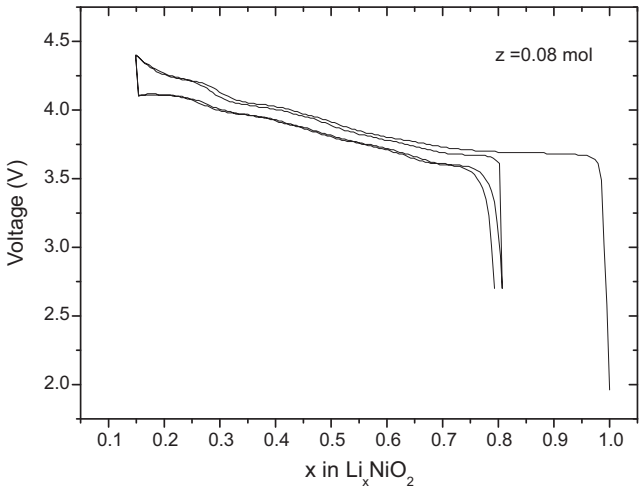

Fig. 1. The 1st and 2nd charge–discharge curves of $LiNiO_2$ synthesized with excess lithium $z = 0.08$ (0.1 C rate, voltage range 2.7–4.4 V, weight ratio of active material:acetylene black:binder = 85:10:5).

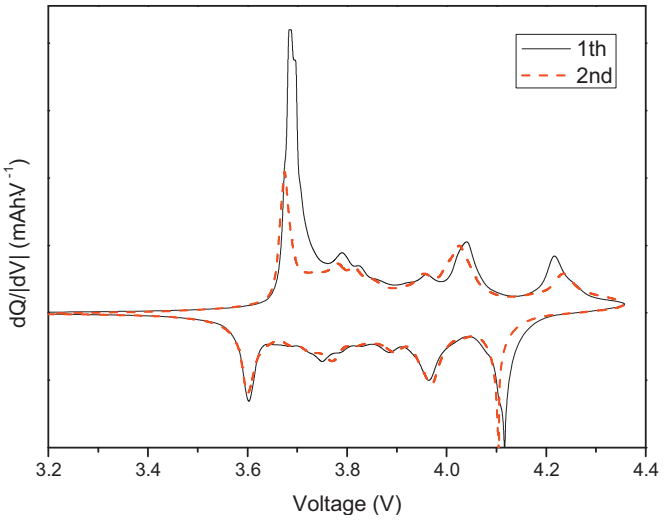

Fig. 2. $dQ/|dV|$ vs. V curves of the 1th and 2nd charge–discharge cycles for $LiNiO_2$ synthesized with excess lithium $z = 0.08$.

discharge capacity, which is revealed by the difference in x of the first charge and discharge curves. The charge and discharge curves exhibit several plateaus in the charge and discharge curves. This indicates that phase transitions occur at several different voltages in the electrode with $z = 0.08$.

$dQ/|dV|$ vs. V curves of the 1th and 2nd charge–discharge cycles for $LiNiO_2$ synthesized with the amount of excess lithium $z = 0.08$ are presented in Fig. 2. Here Q is the charge capacity and V is the voltage. It is reported that phase transitions occur from a hexagonal structure phase to a monoclinic structure phase or vice versa, and from a hexagonal structure phase to another hexagonal structure phase or vice versa during charging and discharging of $LiNiO_2$ [14–16]. The $dQ/|dV|$ vs. V curves show several peaks, indicating that phase transitions occur at several different voltages in the electrode with $z = 0.08$.

The variation of discharge capacity vs. number of cycles n curve with the amount of excess lithium z ($z = 0.04$, 0.08, 0.10, 0.12, and 0.15) for the synthesis of $LiNiO_2$ (0.1 C rate, voltage range 2.7–4.4 V, and weight ratio of active material:acetylene black:binder = 85:10:5) is shown in Fig. 3. The excess lithium z corresponds to the value of z in $Li_{1+z}NiO_2$. The sample with $z = 0.10$ has the largest first discharge capacity (195 mAh/g at a rate of 0.1 C), and the discharge capacity of 155 mAh/g at $n = 25$. It shows relatively good cycling performance with the discharge capacity degradation rate of 1.56 mAh/g/cycle. The first discharge capacity decreases in the order of $z = 0.08$, 0.12, 0.15, and 0.04. The samples with $z = 0.08$, 0.10, 0.12, and 0.15 have similar cycling performances. The sample with $z = 0.04$ has the smallest first discharge capacity (158 mAh/g), but has the best cycling performance with the discharge capacity degradation rate of 0.54 mAh/g/cycle.

Fig. 4 presents the variation of the discharge capacity at 0.1 C rate with the number of cycles for the $LiNiO_2$ cathodes with various weight ratios of active material:acetylene black:-binder (voltage range 2.7–4.4 V). The excess lithium amount z for the synthesis of $LiNiO_2$ was 0.10. The sample with the weight ratio of active material:acetylene black:bin-

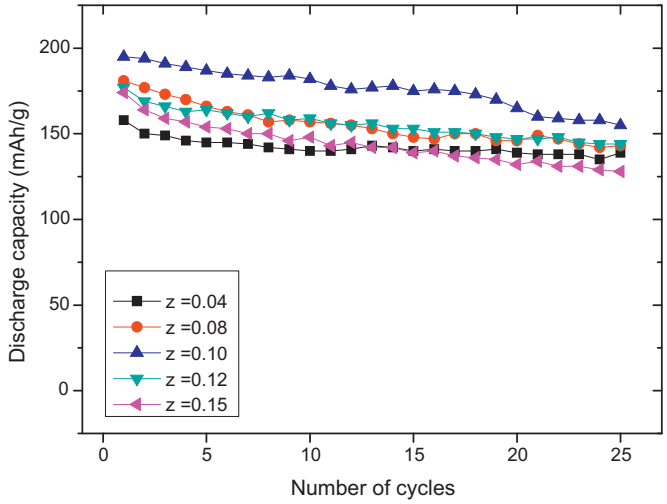

Fig. 3. Variation of discharge capacity vs. number of cycles curve with the amount of excess lithium z (z = 0.04, 0.08, 0.10, 0.12, and 0.15) to synthesize $LiNiO_2$ (0.1 C rate, voltage range 2.7–4.4 V, and weight ratio of active material:acetylene black:binder = 85:10:5).

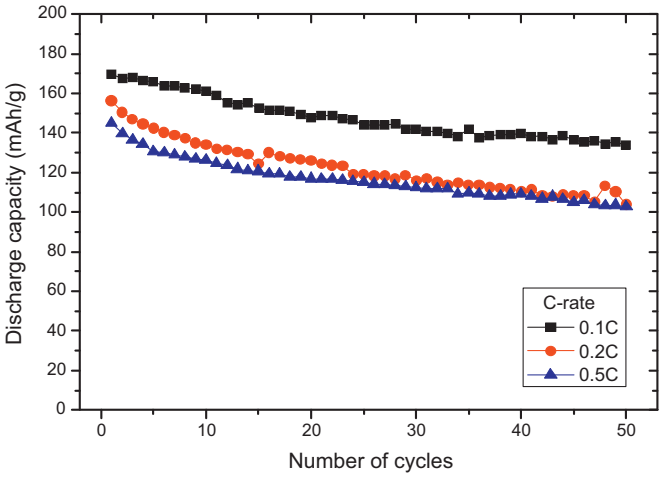

Fig. 5. Variation, with C-rate, of discharge capacity vs. number of cycles curve for the $LiNiO_2$ (synthesized with excess lithium amount z = 0.10) cathode with the weight ratio of active material:acetylene black:binder = 85:10:5 (voltage range 2.7–4.4 V).

der = 85:10:5 has the largest first discharge capacity of 170 mAh/g at a rate of 0.1 C, and the first discharge capacity decreases in the order of weight ratio of active material:acetylene black:binder 85:12:3 and 90:7:3. The cycling performances of the cathodes with different ratios of active material:acetylene black:binder are similar, but the cathode with the ratio of active material:acetylene black:binder 85:10:5 has the smallest discharge capacity degradation rate of 0.70 mAh/g/cycle and the largest discharge capacity at n = 50 of 134 mAh/g. This shows that the cathode with the ratio of active material:acetylene black:binder 85:10:5 has the best electrochemical properties.

The variation, with C-rate, of the discharge capacity vs. number of cycles curve for the $LiNiO_2$ cathode with the weight ratio of active material:acetylene black:binder = 85:10:5 (voltage range 2.7–4.4 V) is given in Fig. 5. The excess

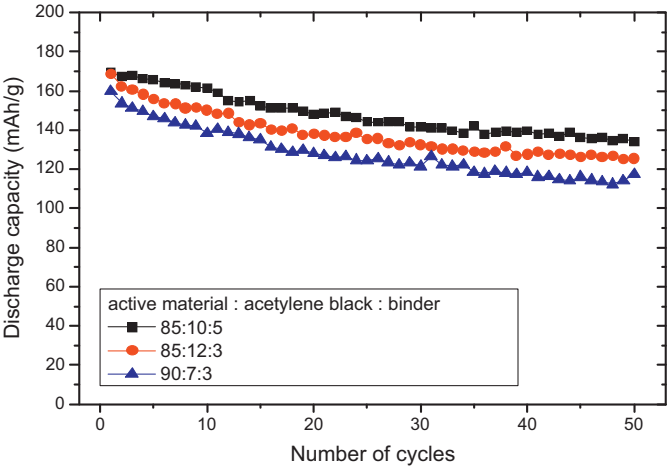

Fig. 4. Variation of the discharge capacity at 0.1 C rate with the number of cycles for the $LiNiO_2$ (synthesized with excess lithium amount z = 0.10) cathodes with various weight ratios of active material:acetylene black:binder (voltage range 2.7–4.4 V).

lithium amount z for the synthesis of $LiNiO_2$ was 0.10. The $LiNiO_2$ cathode has the largest first discharge capacity of 170 mAh/g at a rate of 0.1 C. The first discharge capacity decreases as the C-rate increases. The $LiNiO_2$ cathode exhibits the lowest discharge capacity degradation rate (0.66 mAh/g/cycle) and a discharge capacity at n = 50 of 103 mAh/g at 0.5 C rate. The $LiNiO_2$ cathode has a largest discharge capacity at n = 50 of 134 mAh/g and the discharge capacity degradation rate of 0.70 mAh/g/cycle at 0.1 C rate.

Fig. 6 shows the XRD patterns before cycling and after charge–discharge cycles at 0.1 C, 0.2 C, and 0.5 C rates of the $LiNiO_2$ synthesized with excess lithium amount z = 0.10 (voltage range 2.7–4.4 V, and weight ratio of active material:acetylene black:binder = 85:10:5). All the samples possess the α-$NaFeO_2$ structure of the rhombohedral system (space group; $R\bar{3}m$) with no evidence of any impurities. The XRD patterns of the $LiNiO_2$ after 50 charge–discharge cycles at 0.1 C, 0.2 C, and 0.5 C rates are very similar. They have weaker peaks than that of the $LiNiO_2$ before cycling, indicating that the crystallinity of the $LiNiO_2$ as prepared becomes poor after charge–discharge cycling.

Ohzuku et al. [15] reported that electrochemically reactive $LiNiO_2$ showed a larger integrated intensity ratio of the 0 0 3 peak to the 1 0 4 peak ($I_{0\,0\,3}/I_{1\,0\,4}$) and a clear split of the 1 0 8 and 1 1 0 peaks in its XRD patterns. The degree of cation mixing (displacement of nickel and lithium ions) is low if the value of $I_{0\,0\,3}/I_{1\,0\,4}$ is large and the 1 0 8 and 1 1 0 peaks are split clearly. The value of $(I_{0\,0\,6} + I_{1\,0\,2})/I_{1\,0\,1}$, called the R-factor, is known to decrease as the unit cell volume of $Li_yNi_{2-y}O_2$ decreases. The R-factor increases as y in $Li_yNi_{2-y}O_2$ decreases for y near 1. This indicates that the R-factor increases as the degree of cation mixing becomes larger [7].

Table 1 presents the values of a, c, c/a, unit cell volume, $I_{0\,0\,3}/I_{1\,0\,4}$ and R-factor before cycling and after 50 charging–discharging cycles at 0.1 C, 0.2 C, and 0.5 C rates of the $LiNiO_2$

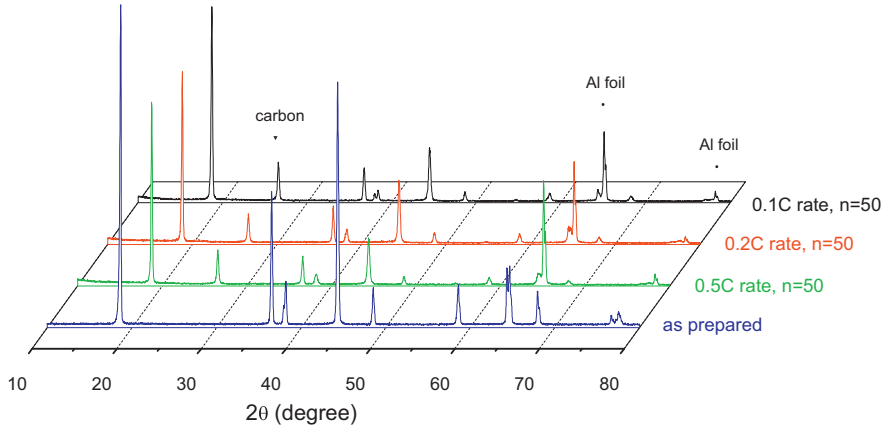

Fig. 6. XRD patterns before cycling and after 50 charge–discharge cycles at 0.1 C, 0.2 C, and 0.5 C rates of the $LiNiO_2$ synthesized with excess lithium amount $z = 0.10$ (voltage range 2.7–4.4 V, and weight ratio of active material:acetylene black:binder = 85:10:5).

Table 1
Values of a, c, c/a, unit cell volume, $I_{0\,0\,3}/I_{1\,0\,4}$ and R-factor before cycling and after 50 charging–discharging cycles at 0.1 C, 0.2 C, and 0.5 C rates of the $LiNiO_2$ synthesized with excess lithium amount $z = 0.10$ (voltage range 2.7–4.4 V, and weight ratio of active material:acetylene black:binder = 85:10:5).

Samples	a (Å)	c (Å)	c/a	Unit cell volume (Å^3)	$I_{0\,0\,3}/I_{1\,0\,4}$	R-factor $[(I_{0\,0\,6}+I_{1\,0\,2})/I_{1\,0\,1}]$
As prepared	2.881	14.209	4.932	102.146	1.319	0.459
0.1 C, $n = 50$	2.874	14.205	4.943	101.600	3.639	0.524
0.2 C, $n = 50$	2.879	14.169	4.922	101.712	2.754	0.605
0.5 C, $n = 50$	2.878	14.186	4.930	101.732	3.905	0.663

synthesized with excess lithium amount $y = 0.10$ (voltage range 2.7–4.4 V, and weight ratio of active material:acetylene black:binder = 85:10:5). The $LiNiO_2$ samples after $n = 50$ have smaller unit cell volume than the as-prepared $LiNiO_2$ sample. The $LiNiO_2$ samples after $n = 50$ have larger $I_{0\,0\,3}/I_{1\,0\,4}$ values and R-factors than the as-prepared $LiNiO_2$ sample. The variations of unit cell volume, $I_{0\,0\,3}/I_{1\,0\,4}$ value and R-factor with cycling may not be used to explain the magnitude of the

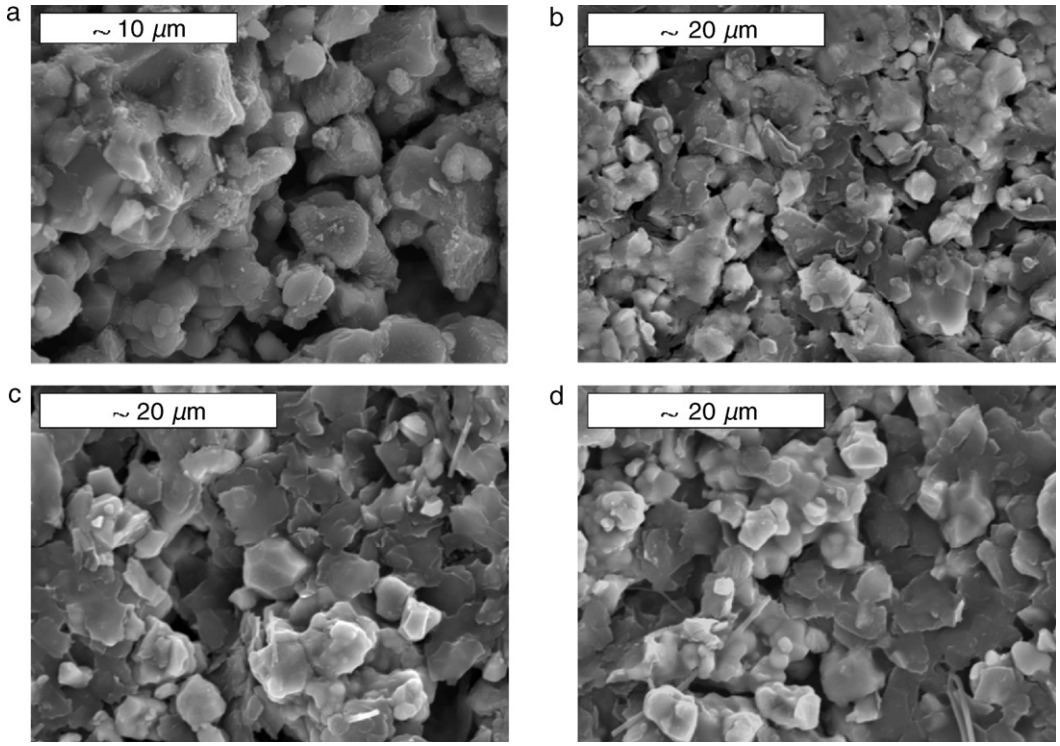

Fig. 7. SEM images (a) before cycling, and after 50 charging–discharging cycles; (b) at 0.1 C rate, (c) at 0.2 C rate, and (d) at 0.5 C rate (voltage range 2.7–4.4 V, and weight ratio of active material:acetylene black:binder = 85:10:5) for the $LiNiO_2$ synthesized with excess lithium amount $z = 0.10$.

discharge capacity after $n = 50$ by relating them to cation mixing because the trends of these values are not general one; The cation mixing decreases, in general, as $I_{0\,0\,3}/I_{1\,0\,4}$ value increases and as unit cell volume and *R*-factor decrease [7,15]. The $LiNiO_2$ sample cycled at 0.1 C rate, with a largest discharge capacity at $n = 50$ of 134 mAh/g (Fig. 5), has the largest *c*/*a* value, the smallest unit cell volume, a relatively large $I_{0\,0\,3}/I_{1\,0\,4}$ value and the smallest *R*-factor, compared with the $LiNiO_2$ samples cycled at 0.2 C and 0.5 C rates.

The SEM images (a) before cycling, and after 50 charging–discharging cycles; (b) at 0.1 C rate, (c) at 0.2 C rate, and (d) at 0.5 C rate (voltage range 2.7–4.4 V, and weight ratio of active material:acetylene black:binder = 85:10:5) for the $LiNiO_2$ synthesized with excess lithium amount $z = 0.10$ are exhibited in Fig. 7. The particles become smaller after charge–discharge cycling. The $LiNiO_2$ cathode cycled at 0.1 C rate has a larger number of small particles and thinner particles with sharper edges, as compared with the $LiNiO_2$ cathode cycled at 0.2 C and 0.5 C rates.

Fig. 8 presents the variation of the image by secondary electron, and the distributions of acetylene black (carbon) and nickel by EDS (energy dispersive spectroscopy) for the $LiNiO_2$ cathode after 50 charge–discharge cycles with the weight ratio of active material:acetylene black:binder. The sample with active material:acetylene black:binder = 85:12:3, which has relatively larger content of acetylene black, exhibits more bright points of carbon than the sample with active material:acetylene black:binder = 90:7:3. All the three samples show the homogeneous distribution of carbon. On the other hand, Ni is not distributed homogeneously in all the samples. This is considered due to the roughness of the sample surface of $LiNiO_2$ containing Ni.

In order to calculate the crystallite size and the strain of the $LiNiO_2$ samples as prepared and after $n = 50$ at 0.1 C rate, the Williamson–Hall method [17] is applied in which the following equation was used:

$$B\cos\theta = \frac{K\lambda}{t} + 4\varepsilon\sin\theta \quad (1)$$

where *B* is full width at half maximum, *K* shape factor(0.9), λ wavelength(1.54056 Å), *t* crystallite size, and ε strain. The $B\cos\theta$ vs. $\sin\theta$ plots to calculate the crystallite size and the strain of the $LiNiO_2$ samples as prepared and after $n = 50$ at 0.1 C rate are shown in Fig. 9. They have the crystallite sizes of 45.0 and 46.4 nm, and the strains of 0.04 and 0.11%, respectively. The crystallite sizes of the $LiNiO_2$ samples as prepared and after

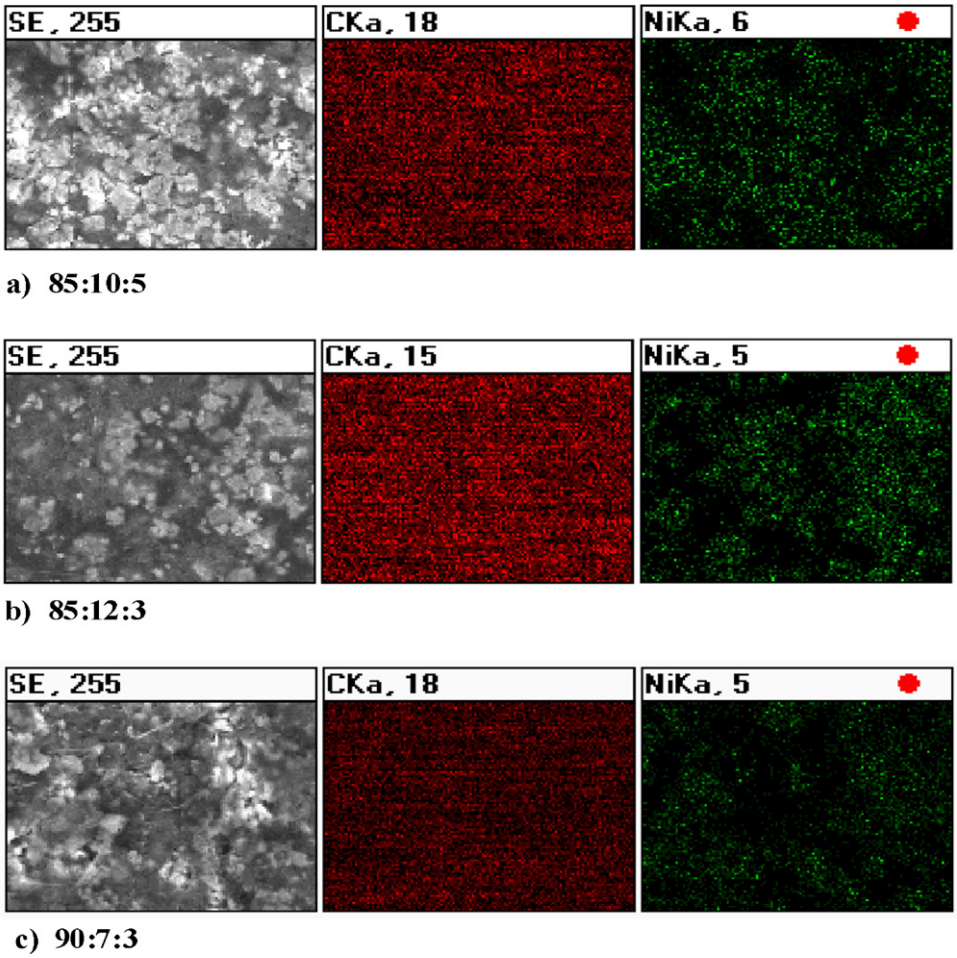

Fig. 8. Variation of image by secondary electron, and distributions of acetylene black (carbon) and nickel for the $LiNiO_2$ cathode with the weight ratio of active material:acetylene black:binder after 50 charge–discharge cycles.

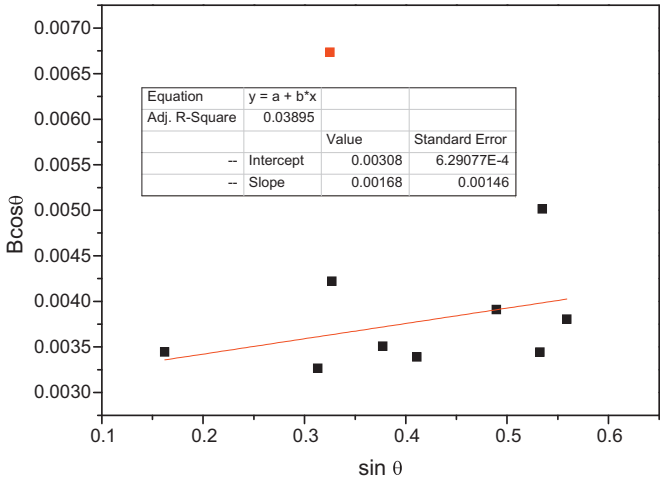

(a) as prepared

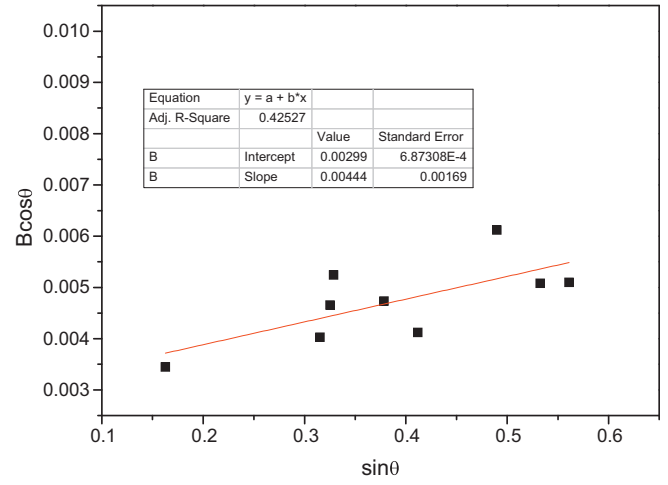

(b) after n=50

Fig. 9. B cos θ vs. sin θ plot to calculate the crystallite size and the strain of the $LiNiO_2$ samples as prepared and after $n = 50$ at 0.1 C rate.

$n = 50$ are practically equal. The results show that the charge–discharge cycling increased the strain. The expansion and contraction of the lattice due to the intercalation and deintercalation with the charge–discharge cycling is considered to increase the strain.

4. Conclusions

The variation of discharge capacity vs. number of cycles curve, with the amount of excess lithium z ($z = 0.04$, 0.08, 0.10, 0.12, and 0.15) to synthesize $LiNiO_2$ (0.1 C rate, voltage range 2.7–4.4 V, weight ratio of active material:acetylene black:binder = 85:10:5) was investigated. The sample with $z = 0.10$ has the largest first discharge capacity (195 mAh/g). The variations of the discharge capacity at 0.1 C rate with the number of cycles for the $LiNiO_2$ cathodes with various weight ratios of active material:acetylene black:binder showed that the cathode with the ratio of active material:acetylene black:binder 85:10:5 has the best electrochemical properties. The variation, with C-rate, of discharge capacity vs. number of cycles curve for the $LiNiO_2$ cathode with the weight ratio of active material:acetylene black:binder = 85:10:5 was investigated. The $LiNiO_2$ cathode has the largest first discharge capacity, the discharge capacity degradation rate of 0.70 mAh/g/cycle and a discharge capacity at $n = 50$ of 134 mAh/g at 0.1 C rate. The crystallite sizes, calculated by the Williamson-Hall method, of the $LiNiO_2$ samples as prepared and after $n = 50$ at 0.1 C rate are practically equal, and the charge–discharge cycling increased the strain.

References

[1] J.M. Tarascon, E. Wang, F.K. Shokoohi, W.R. McKinnon, The spinel phase of lithium manganese oxide ($LiMn_2O_4$) as a cathode in secondary lithium cells, J. Electrochem. Soc. 138 (10) (1991) 2859–2864.
[2] A.R. Armstrong, P.G. Bruce, Synthesis of layered $LiMnO_2$ as an electrode for rechargeable lithium batteries, Lett. Nat. 381 (6582) (1996) 499–500.
[3] M.Y. Song, D.S. Ahn, Improvement in the cycling performance of $LiMn_2O_4$ by the substitution of Fe for Mn, Solid State Ionics 112 (3,4) (1998) 245–248.
[4] K. Ozawa, Lithium-ion rechargeable batteries with $LiCoO_2$ and carbon electrodes: the $LiCoO_2$/C system, Solid State Ionics 69 (3–4) (1994) 212–221.
[5] R. Alcátara, P. Lavela, J.L. Tirado, R. Stoyanova, E. Zhecheva, Structure and electrochemical properties of boron-doped $LiCoO_2$, J. Solid State Chem. 134 (2) (1997) 265–273.
[6] Z.S. Peng, C.R. Wan, C.Y. Jiang, Synthesis by sol–gel process and characterization of $LiCoO_2$ cathode materials, J. Power Sources 72 (2) (1998) 215–220.
[7] J.R. Dahn, U. von Sacken, C.A. Michal, Structure and electrochemistry of lithium nickel oxide ($Li_{1-y}NiO_2$ and a new Li_2NiO_2) phase with the nickel hydroxide ($Ni(OH)_2$) structure, Solid State Ionics 44 (1–2) (1990) 87–97.
[8] J.R. Dahn, U. von Sacken, M.R. Jukow, H. Aljanaby, Rechargeable lithium nickel oxide ($LiNiO_2$)/carbon cells, J. Electrochem. Soc. 138 (8) (1991) 2207–2211.
[9] A. Marini, V. Massarotti, V. Berbenni, D. Capsoni, R. Riccardi, E. Antolini, B. Passalacqua, On the thermal stability and defect structure of the solid solution lithium nickel oxide, Solid State Ionics 45 (1–2) (1991) 143–155.
[10] W. Ebner, D. Fouchard, L. Xie, The $LiNiO_2$/carbon lithium-ion battery, Solid State Ionics 69 (3–4) (1994) 238–256.
[11] Y. Nishida, K. Nakane, T. Satoh, Synthesis and properties of gallium-doped $LiNiO_2$ as the cathode material for lithium secondary batteries, J. Power Sources 68 (2) (1997) 561–564.
[12] J. Morales, C. Perez-Vicente, J.L. Tirado, Cation distribution and chemical deintercalation of lithium nickel oxide ($Li_{1-x}Ni_{1+x}O_2$), Mater. Res. Bull. 25 (5) (1990) 623–630.
[13] M.Y. Song, I.K. Kwon, H.U. Kim, S. Shim, D.R. Mumm, Synthesis of $LiNiO_2$ cathode by the combustion method, J. Appl. Electrochem. 36 (7) (2006) 801–805.
[14] W. Li, J.N. Reimers, J.R. Dahn, In situ X-ray diffraction and electrochemical studies of $Li_{1-x}NiO_2$, Solid State Ionics 67 (1993) 123–130.
[15] T. Ohzuku, A. Ueda, M. Nagayama, Electrochemistry and structural chemistry of lithium nickel oxide ($LiNiO_2$)($R\bar{3}m$) for 4 volt secondary lithium cells, J. Electrochem. Soc. 140 (7) (1993) 1862–1870.
[16] H. Arai, S. Okada, H. Ohtsuka, M. Ichimura, J. Yamaki, Characterization and cathode performance of $Li_{1-x}Ni_{1+x}O_2$ prepared with the excess lithium method, Solid State Ionics 80 (1995) 261–269.
[17] C. Suryanarayana, M. Grant Norton, X-ray Diffraction, A Practical Approach, Plenum Press, New York, 1998, pp. 207–222.